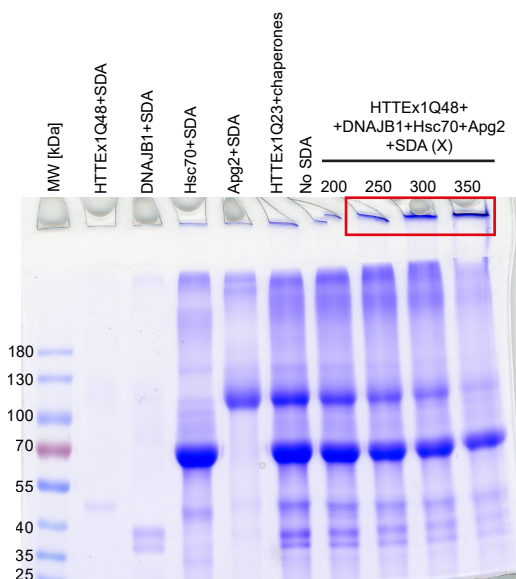
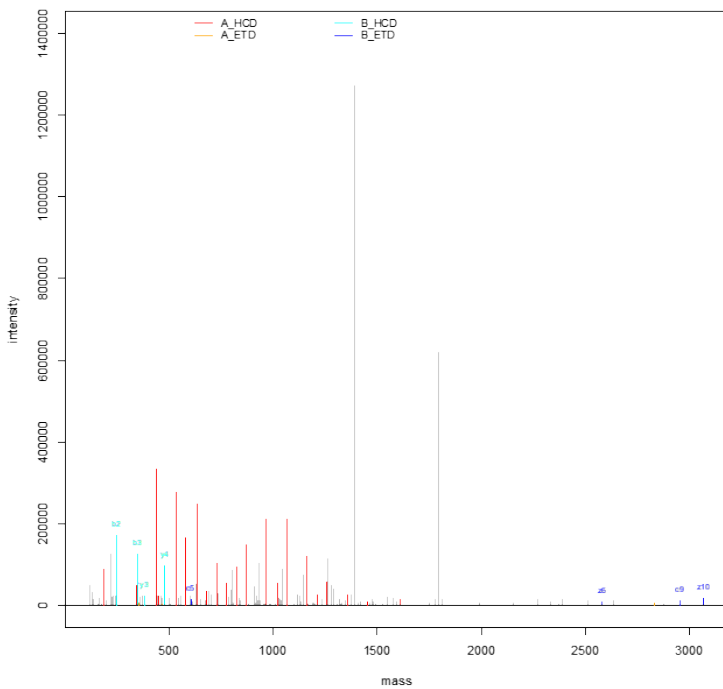


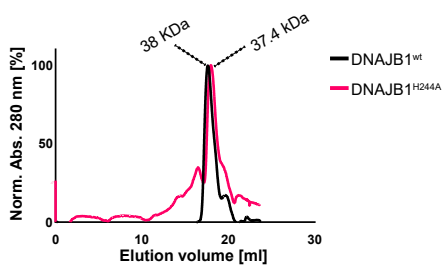
a



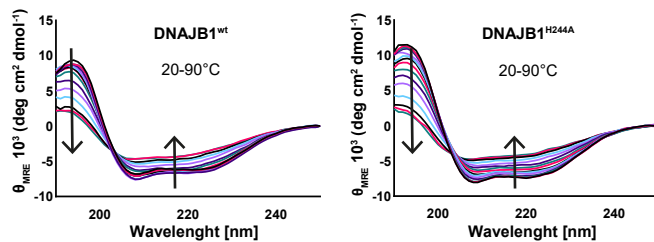
Peptide A: LPQLQPPPPPPPPGPA
Peptide B: VFLKDKPHNI



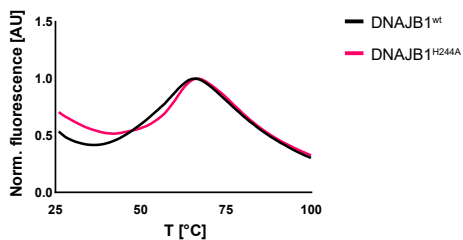
b



d

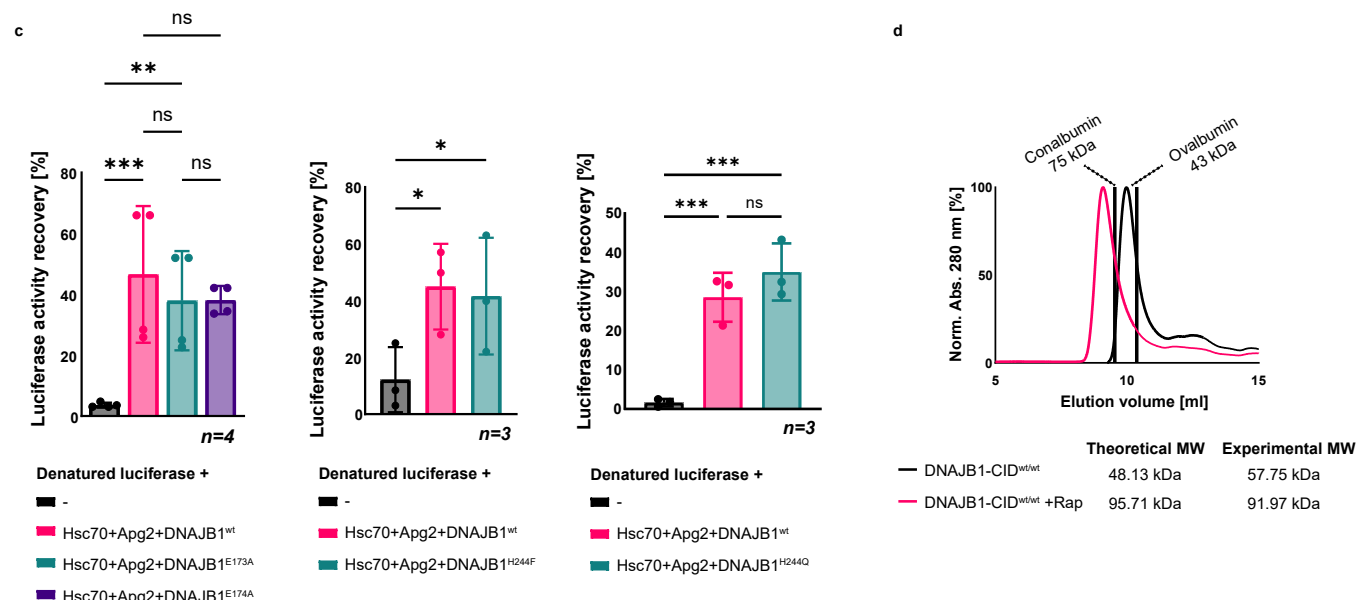
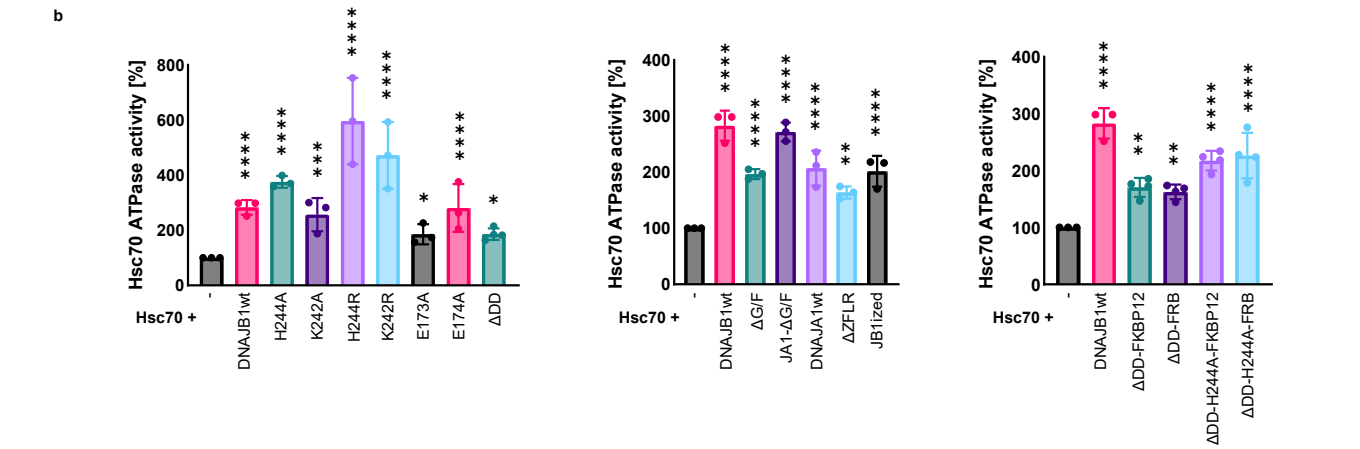
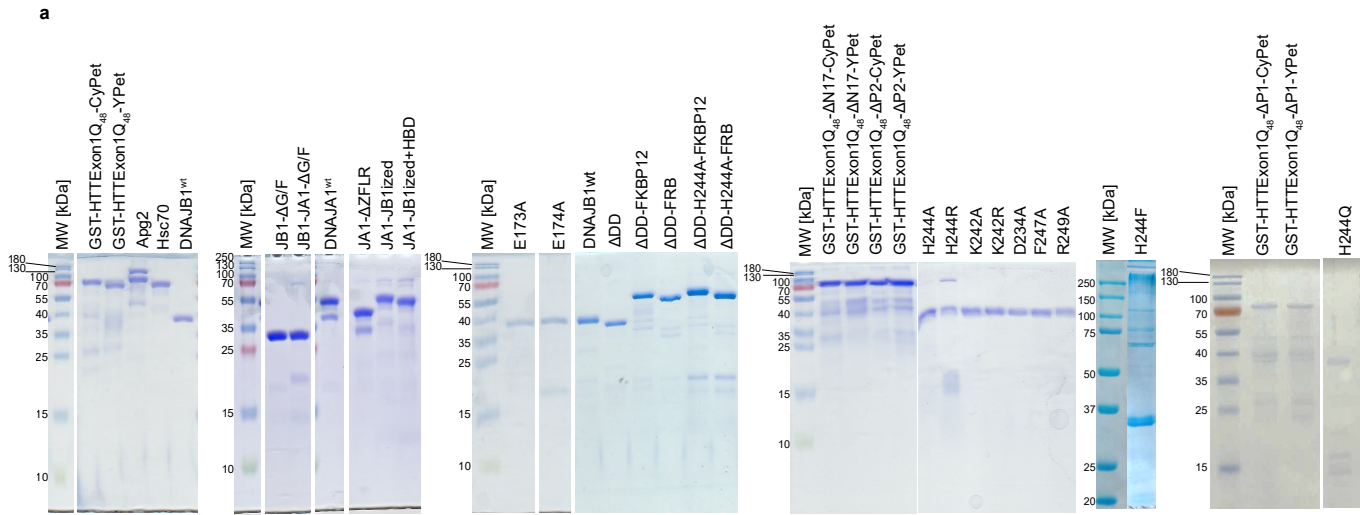


c



Supplementary figure 1. XL-MS analysis and integrity analysis of DNAJB1 variants

a) Left, representative SDS–PAGE of cross-linked proteins. The gel piece highlighted in red box was excised and in-gel digested for LC-MS analysis. We have performed more than ten independent crosslinking analyses of HTTExon1Q_n and the chaperones. The depicted gel is a representative example. Right, the MS2 spectrum of an identified cross-link. **b)** Size exclusion chromatography of DNAJB1^{wt} and DNAJB1^{H244A}. **c)** Melting curve of DNAJB1^{wt} (red) and DNAJB1^{H244A} (black) obtained by differential scanning fluorescence using SYPROorange dye. **d)** Top, CD spectra of DNAJB1^{wt} and DNAJB1^{H244A} obtained over a temperature range of 20-90°C. Bottom, calculation of the melting temperature (T_m), which is defined as $\alpha = 0.5$.



Supplementary figure 2. Analysis of purified proteins and control chaperone assays

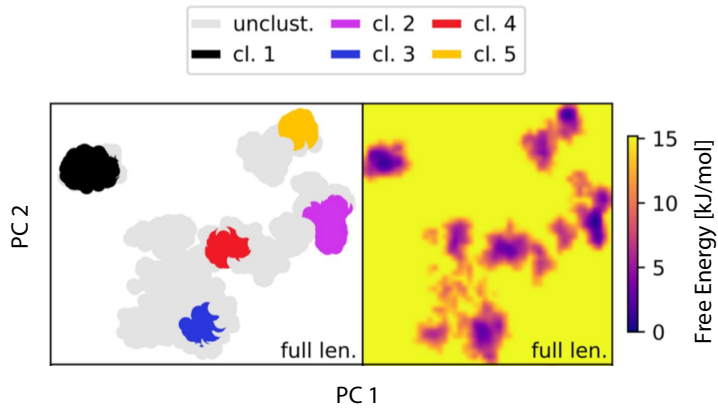
a) SDS-PAGE analysis of all purified proteins used in this study. At least three batches of each protein were independently overexpressed and purified. 15 μ l of 2 μ M of each protein were subjected to SDS-PAGE with subsequent Coomassie staining.

b) ATPase activity of Hsc70 alone and upon addition of DNAJB1^{wt} and variants. Three independent experiments were performed and all data were normalized to the intrinsic ATPase activity of Hsc70. One-way ANOVA analysis was used to evaluate the significance of the difference observed between Hsc70 alone and Hsc70 plus a DNAJB1 variant. The extent of ATPase activation of Hsc70 by the different DNAJB1 variants could be due to altered affinities to Hsc70. Bars represent the mean value and error bars correspond to the mean SD. ****, $p \leq 0,0001$; ***, $p \leq 0,001$; **, $p \leq 0,01$; *, $p \leq 0,1$.

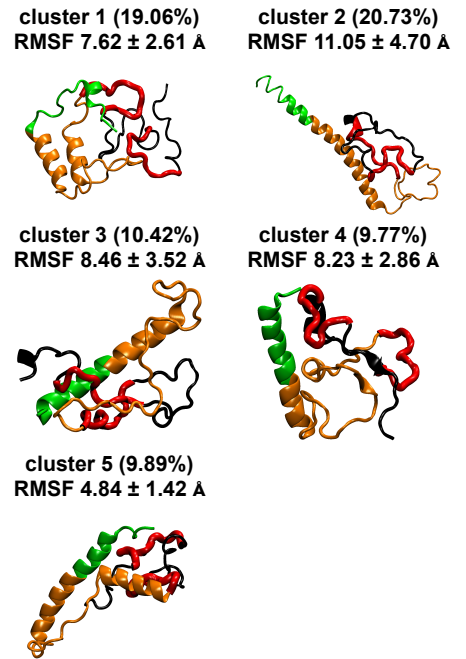
c) Recovered enzymatic activity of luciferase after 2 h incubation with Hsc70, Apg2 and DNAJB1^{wt} or variants E173A, E174A (left), H244F (middle), and H244Q (right). Data from three independent experiments were analyzed with a one-way ANOVA test. Bars represent the mean value and error bars correspond to the mean SD. ***, $p \leq 0,001$; **, $p \leq 0,01$; *, $p \leq 0,1$; ns, not significant.

d) Size exclusion chromatography of DNAJB1 ^{Δ DD}-FKBP12 and DNAJB1 ^{Δ DD}-FRB in the absence (black) or presence (magenta) of Rapamycin. The elution volumes of MW standards Conalbumin and Ovalbumin are indicated on top and were used to calculate the experimental MW of the proteins.

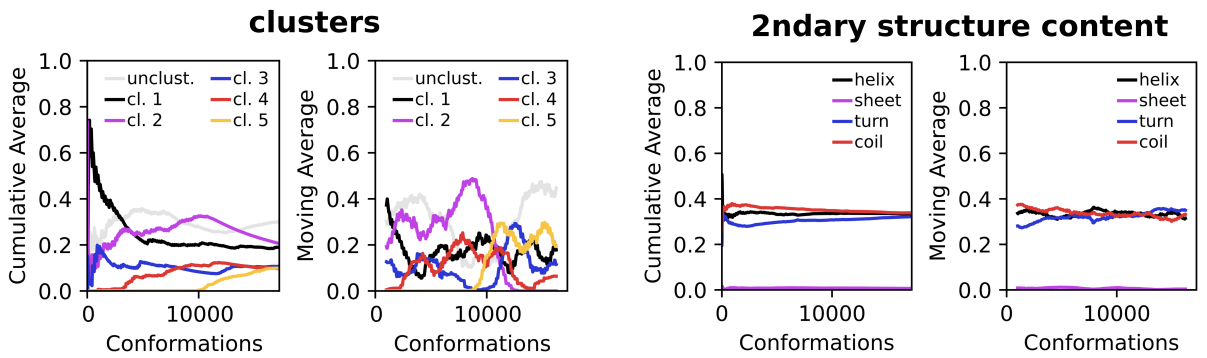
a



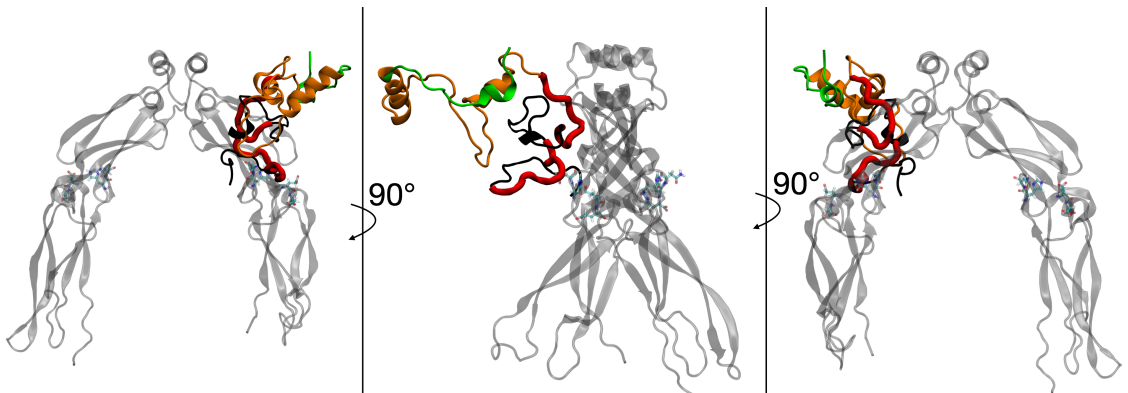
b



c



d



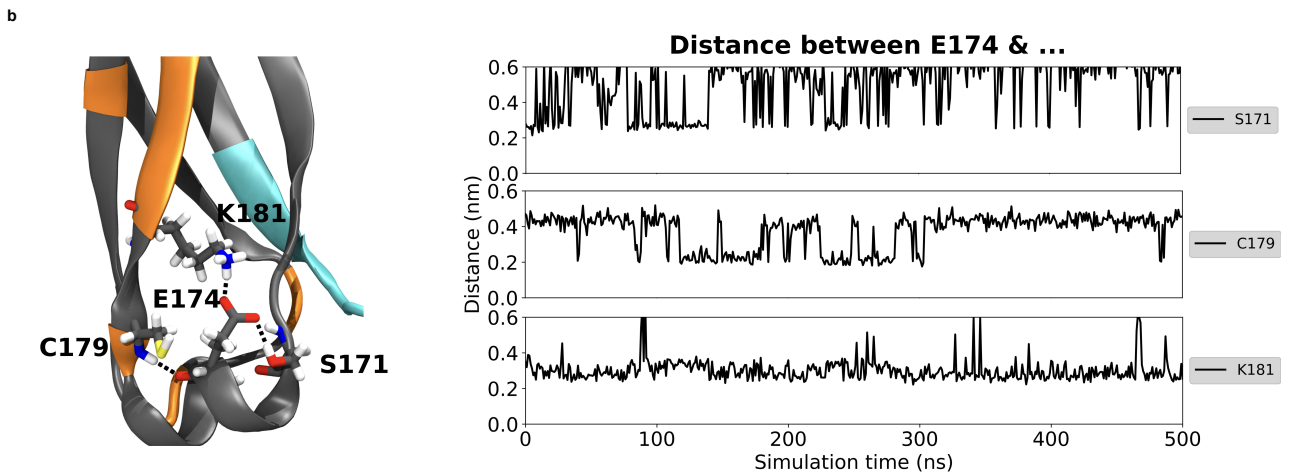
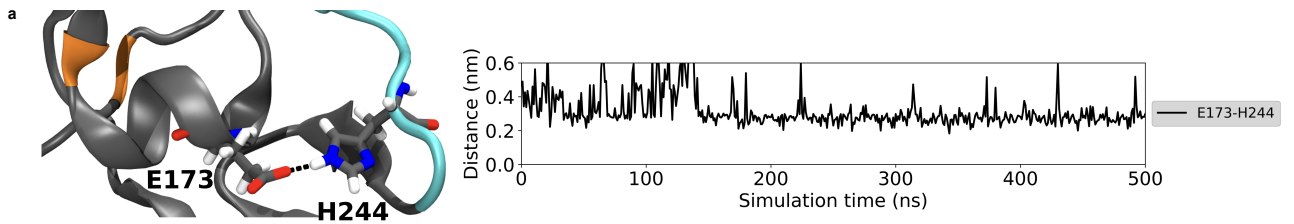
Supplementary figure 3. Structure prediction of HTTExon1Q₄₈ and docking to DNAJB1

a) Dihedral principal component analysis (dPCA) of HTTExon1Q₄₈ with the corresponding density-based clustering analysis. The colors indicate the respective clusters (left) and the free energy in kJ/mol (right).

b) Respective structural clusters determined by dPCA analysis with their probability and root mean square fluctuation (RMSF). The average RMSF values are measured within these clusters comparing the protein backbone atoms to the averaged positions after aligning all conformations to the first structure. The N17 domain is depicted in green, the polyQ stretch in orange, the P1 and P2 of the PRD in red and the residues between P1 and P2 in black.

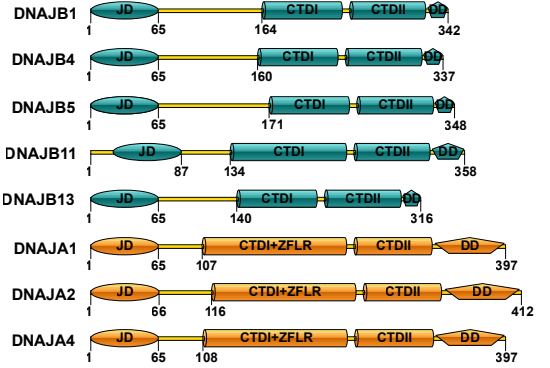
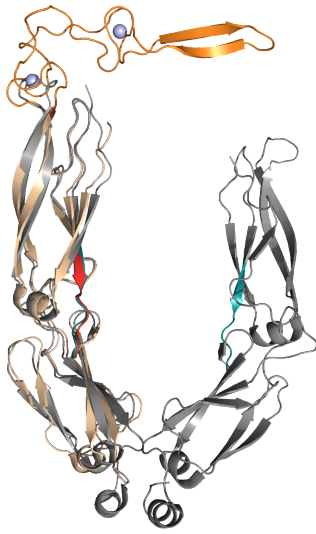
c) Cumulative and moving average fractions for the most populated clusters (left) and the secondary structure content (right). Conformations are ordered after the occurrence time in the base line replica at 310 K. The moving average window size was set to 2000 conformations. The helical content in cluster 1 and cluster 3 converged fast during the replica exchange simulation, while other clusters 2, 4 and 5 converged slower and might have not reached the equilibrium probability within the simulation time.

d) Equilibrated complex of DNAJB1 and HTTExon1Q₄₈ after 320 ns of classical MD simulation. Rotation around the symmetry axis of DNAJB1 reflects binding of HTTExon1Q₄₈ on one protomer only. The binding site on the second protomer is kept free.

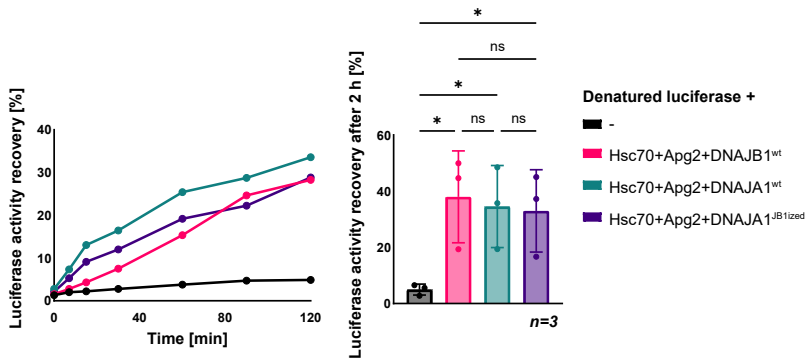


Supplementary figure 4. MD snapshot of the hinge region between CTDI and CTDII **a)** Visualization of the hydrogen bond (black dotted line) between E173 and H244A. The distance between hydrogen bond forming atoms of E173 (center of both oxygens) and H244 were recorded for DNAJB1^{wt} over the simulation time of 500 ns (right panel). **b)** Analogous, the hydrogen bonds between E174 and S171, C179 and K181 are highlighted with black dashed lines in the molecular snapshot and the time evolution over 500 ns plotted. DNAJB1 is represented in cartoon style in gray. Highlighted amino acids of DNAJB1 are represented as licorice style with a coloring code according to the atom types: hydrogen (white), carbon (cyan), oxygen (red), nitrogen (blue). The HBM is colored in cyan.

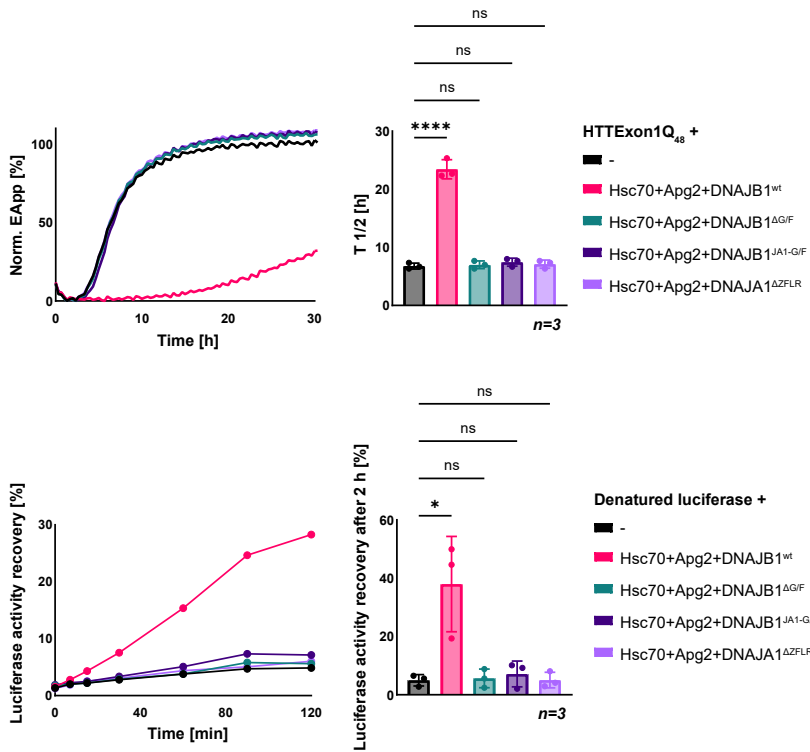
a



b



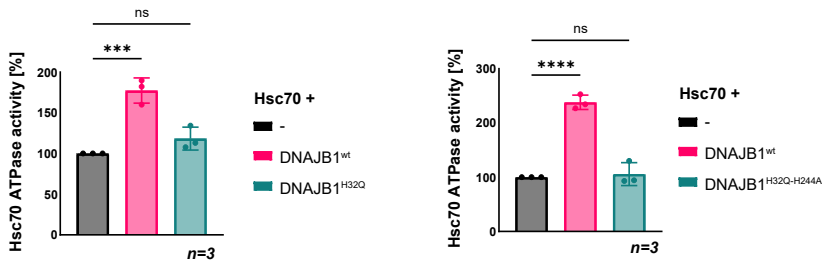
c



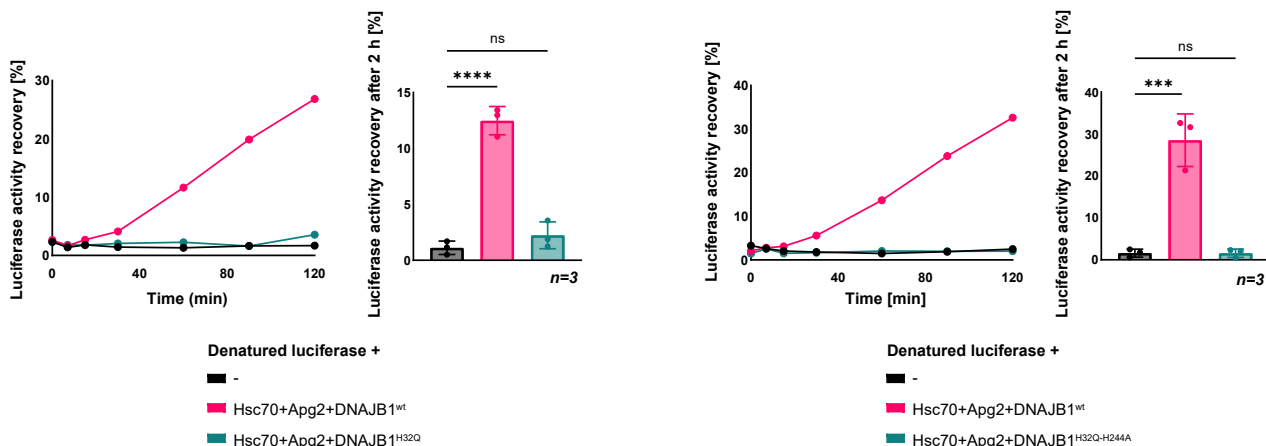
Supplementary figure 5. Domain architecture of different JDPs and analysis of DNAJB1 variants in chaperone assays

a) Left, structural overlay of a dimer of CTDs of DNAJB1^{wt} (in gray) and a monomer of CTD of DNAJA1^{wt} (in sand). The C-terminal domain model of DNAJA1 was build based on the highly homologous CTD of yeast Ydj1 (pdb: 1nlt) using the Prime homology modeling tool of the Maestro Software Suite Version 12.7 (Schrödinger LLC). The most striking difference between the two structures is the protrusion of the ZFLR from the CTDI of DNAJA1^{wt} (in orange). The remaining structures of DNAJB1^{wt} and DNAJA1^{wt} CTDs, including the HBM (green and red β -sheets), overlap. Right, schematic alignment of human J-domain proteins from class A (orange) and class B (teal). The G/F-rich domains (depicted in yellow and connecting the J-domains with the CTDs) of class B J-domain proteins are significantly longer than those of class A J-domain proteins. **b)** Refolding of denatured luciferase by Hsc70, Apg2 and DNAJB1^{wt}, DNAJA1^{wt} or DNAJA1^{JB1ized}. The graph is a representative result of three independent experiments. A one-way ANOVA analysis of the amount of refolded luciferase after 2 h of incubation with chaperones is depicted on the right. Bars represent the mean value and error bars correspond to the mean SD. **, $p < 0,5$; *ns*, not significant. **c)** Effect of Hsc70, Apg2 and DNAJB1^{wt}, DNAJB1 ^{Δ G/F} (deletion of G/F-rich domain), DNAJB1^{JA1-G/F} (G/F-rich domain substituted by the shorter G/F-rich domain of DNAJA1), DNAJA1^{wt} or DNAJA1 ^{Δ ZFLR} (ZFLR deleted) on HTTExon1Q₄₈ aggregation (top) and refolding of heat-denatured luciferase (bottom). The graphs on the left are representative results of three independent experiments. The bar graphs on the right are the one-way ANOVA analysis of the half-life ($T_{1/2}$) of HTTExon1Q₄₈ aggregation (top) and the amount of refolded luciferase after 2 h (bottom). Error bars correspond to the SD. ****, $p \leq 0,0001$; **, $p < 0,5$; *ns*, not significant.

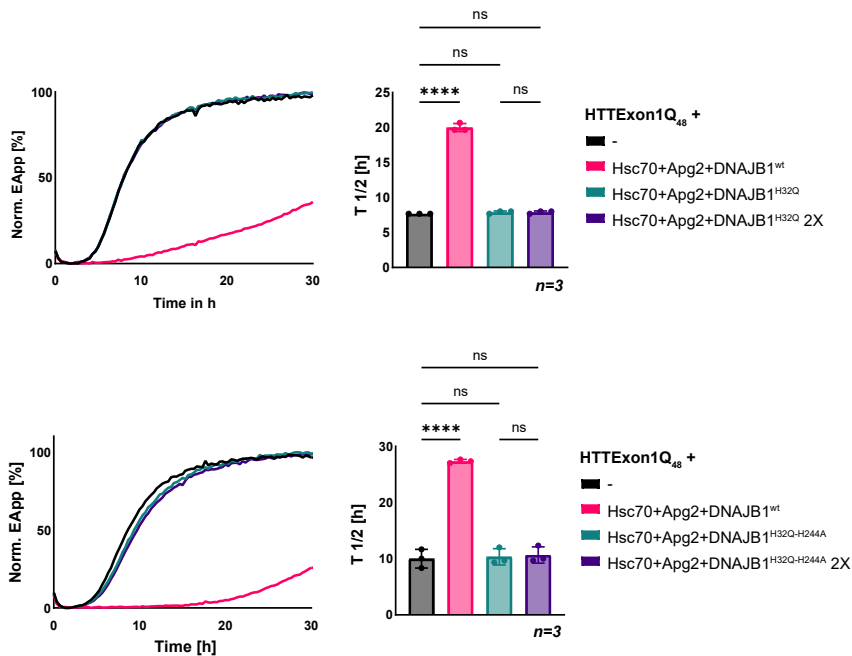
a



b



c

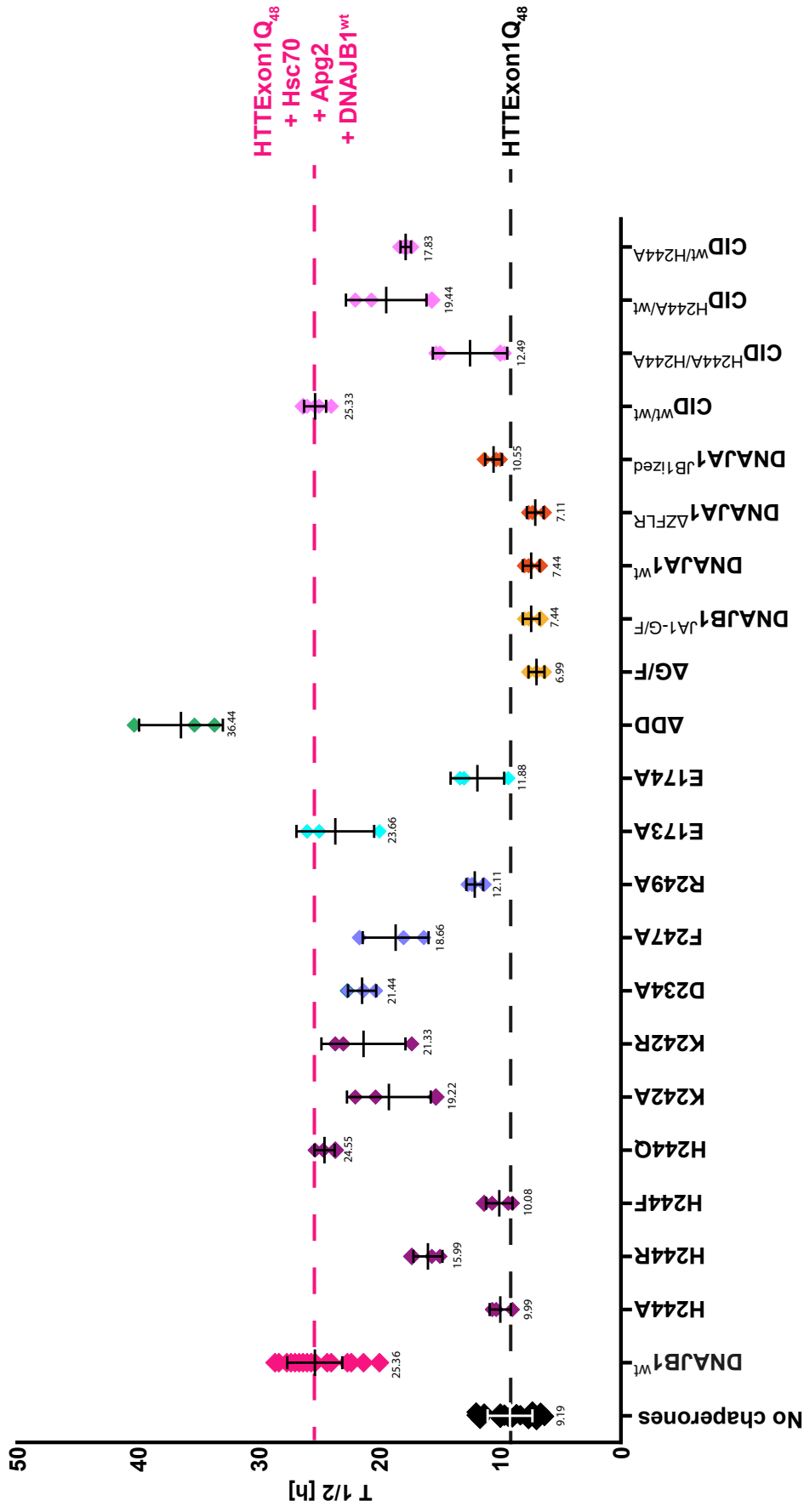


Supplementary figure 6. Analysis of the HPD motif of DNAJB1 in chaperone assays

a) ATPase activity of Hsc70 alone and upon addition of DNAJB1^{H32Q} (left) or DNAJB1^{H32Q-H244A} (right). All data were normalized to the intrinsic ATPase activity of Hsc70. One-way ANOVA analysis was used to evaluate the significance of the difference observed between Hsc70 alone and Hsc70 plus each mutant. Bars represent the mean value and error bars correspond to the mean SD. ****, $p \leq 0,0001$; ***, $p < 0,001$; ns, not significant.

b) Refolding of denatured luciferase by Hsc70, Apg2 and DNAJA1^{H32Q} (top) or DNAJA1^{H32Q-H244A} (bottom). A one-way ANOVA analysis of the amount of refolded luciferase after 2 h of incubation with chaperones is depicted on the right side of each graph. Bars represent the mean value and error bars correspond to the mean SD. ****, $p < 0,0001$; ***, $p \leq 0,001$; ns, not significant.

c) FRET assay of HTTExon1Q₄₈ aggregation and the effect of the addition of Hsc70, Apg2 and DNAJA1^{H32Q} (top) or DNAJA1^{H32Q-H244A} (bottom). The graph is a representative result of three independent experiments and a one-way ANOVA analysis of the half-life ($T_{1/2}$) of HTTExon1Q₄₈ aggregation under the tested conditions is depicted on the right. Error bars correspond to the SD. ****, $p \leq 0,0001$; ns, not significant.



HTTExon1Q₄₈ + Hsc70 + Apg2 +

- ◆ Point mutations on HBM residues
- ◆ Point mutations on HBM flanking region residues
- ◆ Point mutations on HBM interacting residues
- ◆ Deletion of dimerization domain
- ◆ Mutations on G/F-rich region
- ◆ DNAJA1 JB1ization
- ◆ Chemically-induced dimers

Supplementary figure 7. Summary of the $T_{1/2}$ of HTTExon1Q₄₈ fibrilization

Depicted is the $T_{1/2}$ of HTTExon1Q₄₈ upon addition of Hsc70, Apg2 and each of the JDP described in this study (Figs 1, 2, 4, 5, 6, 7 and Supplementary Figure 5). The black dashed line corresponds to the mean $T_{1/2}$ of HTTExon1Q₄₈ fibrilization and the magenta dashed line corresponds to the $T_{1/2}$ of HTTExon1Q₄₈ fibrilization in the presence of Hsc70, Apg2 and DNAJB1^{wt} and ATP regeneration system. Each diamond represents the $T_{1/2}$ of HTTExon1Q₄₈ fibrilization when DNAJB1^{wt} is substituted by the variants shown on the x-axis. Each variant was tested in three independent experiments. The mean $T_{1/2}$ values (in h) are shown below each diamond. The error bars represent the mean SD. The color code of the diamonds indicates the type of variant/mutation used and is listed below the graph.